

Effect of annealing on undoped and Ce, Dy, Eu, Ni-doped ZnO properties synthesized by sol-gel method.

J. Ungula, and F.B. Dejene

Department of Physics, University of the Free State (Qwaqwa), Private Bag x 13,
Phuthaditjhaba, 9866

*Corresponding author e-mail address:dejenebf@qwa.ufs.ac.za

Abstract. In this study, undoped and Ce, Dy, Eu, and Ni-doped zinc oxide (ZnO) was prepared by sol-gel method from zinc acetate, metal nitrates and sodium hydroxide with water and ethanol as solvents and the effects of annealing temperature were investigated. The XRD measurements showed that the synthesized ZnO nanoparticles had the pure wurtzite structure. It is found that with annealing the crystallinity improved and the particle size increases while the band gap energy of the materials decreases. The reflectance spectra of the products show that the percentage absorption in visible range increases with annealing temperature. The SEM micrograph of ZnO revealed that the surface morphology depends on both the dopant used and annealing temperature. Furthermore, PL spectra showed strong, broad and intense emission in visible region for Ce-doped ZnO samples while other dopants suppressed this green emission.

1. Introduction

In the last decade, ZnO has received much attention in view of optoelectronic device applications in the ultraviolet and the visible ranges due to its prominent properties, such as wide band gap (3.37 eV) and high exciton binding energy (60 meV) [1–3]. ZnO is also used in polycrystalline form for facial powder, piezoelectric devices, varistors, phosphors, and transparent conducting oxide films [3]. Besides the UV light-emitting properties, visible luminescence in a range of 400–700 nm for ZnO, was also studied widely because of the potential application in low-voltage field emissive display [4]. On the other hand, the intrinsic properties of ZnO have also been improved by controlling their preparation conditions [5–7]. Doping with selective elements offers an effective method to enhance and control the electrical and optical properties of ZnO nanostructures, which is crucial for its practical application. It is also suggested that annealing at temperatures between 500°C and 700°C leads to an improvement in the crystalline quality (due to the higher UV/DLE intensity ratio compared to the as grown sample). It is expected that at these temperatures, the energy supplied by annealing is sufficient to remove any surface adsorbed impurities and so it becomes energetically favorable for atoms to move into proper sites, leading to an improvement in the crystal quality [8]. In this report the effect of the annealing temperature on the particle size, morphology and photo-luminescence (PL) properties of the synthesized undoped and Ce, Dy, Eu, Ni-doped ZnO nanoparticles were investigated systematically.

2. Experimental

Zinc acetate reacted with sodium hydroxide in a molar ratio of 0.02mol to 0.08mol where the mixture of water and ethanol were used as solvent. For the production of pure ZnO nanostructures solution of NaOH was titrated against Zinc acetate dehydrate slowly and stirred vigorously for 2 hours, and then kept in a cabinet for some hours to form gel-like solution. This was rinsed using heptane and ethanol

mixture, filtered and dried in oven for 1 hour. The dried sample was separated into two portions. The first portion was left to dry further at room temperature and the second portion annealed for 1 hour at 600°C in a furnace (air atmosphere). For the production of doped ZnO nanoparticles, it was performed by adding acetates of Ce, Eu, Dy and Ni to Zinc acetate dehydrate. The mixture so formed was treated through the same procedure for pure ZnO to obtain both the annealed and as prepared samples of the nanoparticles. The molar ratio of dopants to zinc was kept constant at 2%. The structure of ZnO nanoparticles was characterized by XRD on Bruker D8 X-ray diffractometer using Cu K α radiation ($\lambda=1.5406 \text{ \AA}$) in the 2θ range from 20° to 80° . The surface morphology was studied with a SEM using a Shimadzu model SSX-550 superscan Scanning Electron Microscope. PL measurement was performed on a Cary Eclipse fluorescence spectrophotometer; model LS-55 with a built-in 150W xenon flash lamp as the excitation source and a grating to select a suitable excitation wavelength.

3. Results and discussion

3.1 SEM Analysis

SEM micrographs for annealed and variously doped ZnO nanoparticles are shown in the figure 1. Clearly the powders are in the form of agglomerates with non-uniform shapes and sizes caused by the difference in type of dopants. The SEM observation revealed nanorods and nanoparticles of ZnO depending on the dopant used. For calcinations, the particles showed increment in size, because at higher calcinations temperature the particles agglomerate to produce larger particles in size. It was also observed that the sizes of ZnO nanoparticles became bigger with annealing. In Figure 1 (a), Ce-doped ZnO shows relatively larger nanorods

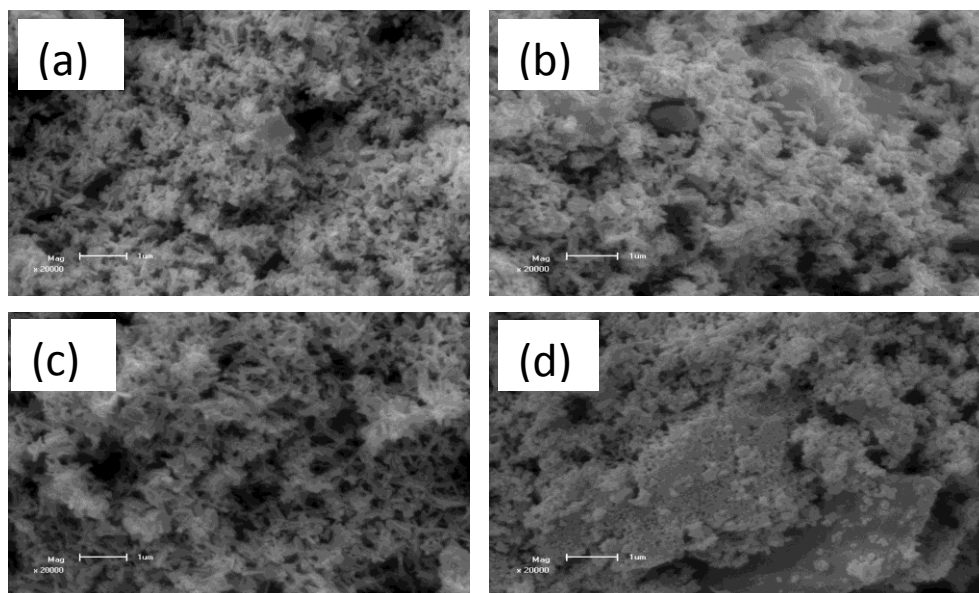


Figure 1: SEM images of annealed (a) Ce-doped ZnO (b) Eu-doped ZnO (c) Dy-doped ZnO (d) Ni-doped ZnO nanostructures.

3.2 XRD Analysis

The information about the crystal structure and the shape of ZnO nanostructures were obtained from XRD measurements. Figures 2 and 3 show that the diverse morphologies observed by SEM and the presence of the doping species do not seem to have an influence on the crystalline phase of the different samples. As revealed by XRD analysis, all ZnO nanostructures, either undoped or doped,

show the typical hexagonal wurtzite structure (with respect to the standard card-JCPDS No. 36-1451), and the sharp diffraction peaks indicate the formation of highly crystalline nanostructures. It was found that with annealing the crystallinity of the samples improved and particle sizes increase as shown by the increased intensity of peaks and narrowing of peak widths, respectively according to Fig. 2(a), while decreased peak intensity and broadening of peak width was observed for unannealed samples as shown in Fig 2(b). The crystallite size of as-prepared doped ZnO nanoparticles calculated using the Debye Scherer formula are in the range of 31.3 - 38 nm, while that of the annealed ZnO nanoparticles are in the range 31.4 - 39.1 nm. There is no substantial increase in grain size after annealing for 1 hour at 600°C. Apparently, the annealing time is too short to cause an appreciable increase in the grain size. The improvement of crystallinity after annealing may be due to defect healing and removal of adsorbed impurities as is stated earlier. This proves that the temperature has a slight impact on the crystalline size of ZnO nanoparticles as increase in annealing temperature enhances the kinetic energy of the reaction system, and subsequently increases the number of particle collisions. The increase in particle collision decreases time to reach a stable size. According to aggregation theory time to reach a stable size is inversely proportional to particle size [9]. Therefore the particle size increases with annealing temperature.

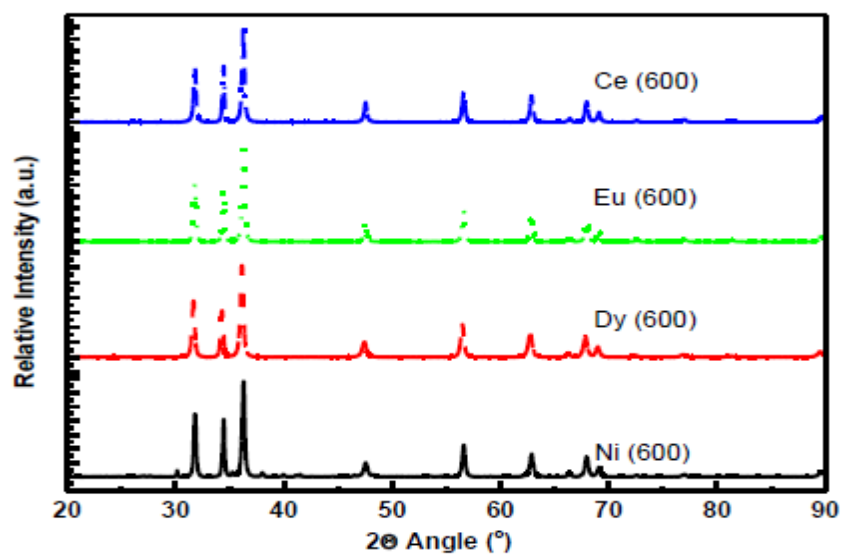


Figure 2 (a): XRD spectra of annealed doped ZnO nanoparticles

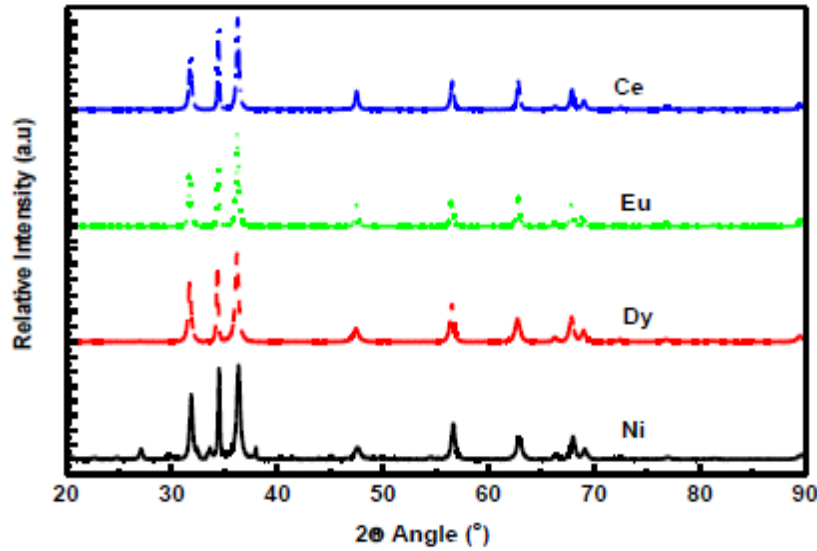


Figure 2 (b): XRD spectra of unannealed doped ZnO nanoparticles

3.3 Photoluminescence

Figure 3 shows the PL measurements recorded with excitation wavelength set at 364 nm. The undoped ZnO sample exhibits a weaker emission band at 380 nm and a broad intense band at around 560 nm in the UV and visible region, respectively. The near-band-edge (NBE) emission in the UV region is attributed to the recombination of free excitons, while the broad green emission is believed to be related to deep levels caused by intrinsic defects such as oxygen vacancies, Zn interstitials, or their complexes [10, 11]. The intrinsic luminescence spectrum of ZnO may vary slightly from sample to sample depending on the syntheses and processing conditions, but it always occurs in the green region of the spectrum. Emission of Eu-doped ZnO demonstrates a broad emission band at 554 nm in the visible range due to Eu^{2+} as a result of the $f-d$ transition [12]. A weaker emission appearing at ~ 618 nm is ascribed to the Eu^{3+} emission. The PL emission of Ce^{3+} -doped ZnO depicts broad emissions in the visible region. Two luminescence bands contribute to this two broad band with the maximum at 504 and 538 nm. It is well known that the emission from Ce^{3+} is either in the UV or visible region, consisting typically of two main luminescent centres [13] which corresponds to the transitions from the lowest $5d$ crystal field component (${}^2D_{3/2}$) to the two components (${}^2F_{5/2}$ and ${}^2F_{7/2}$) of the $4f$ ground state. The PL emission spectra from $\text{ZnO}:\text{Ce}^{3+}$ is very similar to that of ZnO but with slight blue shift. Evidently, the positions and intensities of the PL peaks were both affected by annealing temperature as the intensity of emission peaks of the undoped and doped-ZnO nanoparticles increase with annealing temperature. This shift of band-gap energy was believed to originate from the change of tensile stress because of lattice distortion. Similarly, the visible luminescence of ZnO nanoparticles increases with annealing. No emission bands were observed for Dy and Ni-doped ZnO samples.

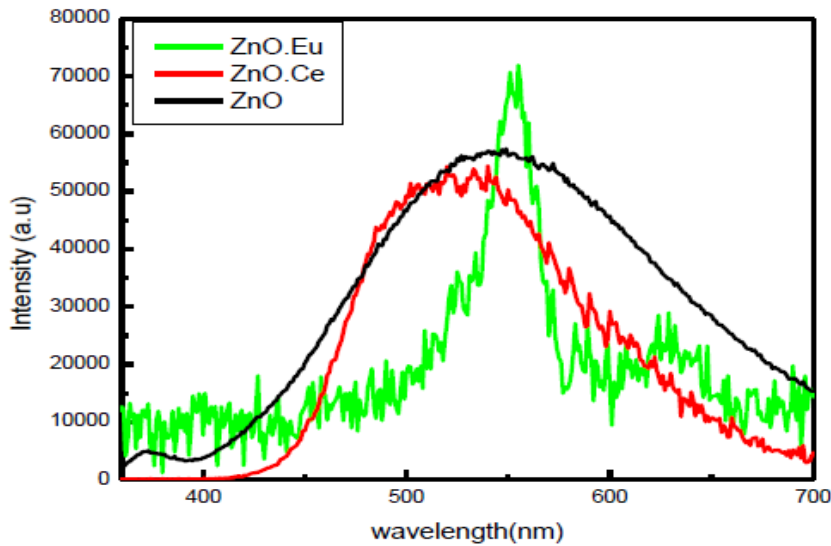


Figure 3: PL of undoped ZnO, Ce and Eu-doped ZnO nanoparticles

3.4 Optical properties

The absorption of the ZnO was obtained using the UV-Visible spectra. In general, absorption spectra probe the crystallite internal molecular orbital and provide information concerning size and particle composition [9]. Figure 4(a) shows the optical reflectance spectra of doped ZnO nanostructures. The UV measurements depict a slight shift in absorption edge confirming the changes in particle sizes. The energy band gap of these materials was estimated using the Kubelka-Munk function emission function [10] for direct transitions. The band gap energy of the ZnO nanostructures prepared with different types of dopant was found to vary between 2.9 and 3.1 eV as shown in Figure 4(b). The estimated band gap energy is lower than that of bulk ZnO (3.37 eV). This band gap reduction may be due to surface defects density of the synthesised undoped and doped ZnO nanostructures [14]. The absorption in the visible region changed with the changes in types of dopant. Ni-doped ZnO was seen to absorb the largest percentage of excitation energy, while Eu-doped ZnO absorbs the least.

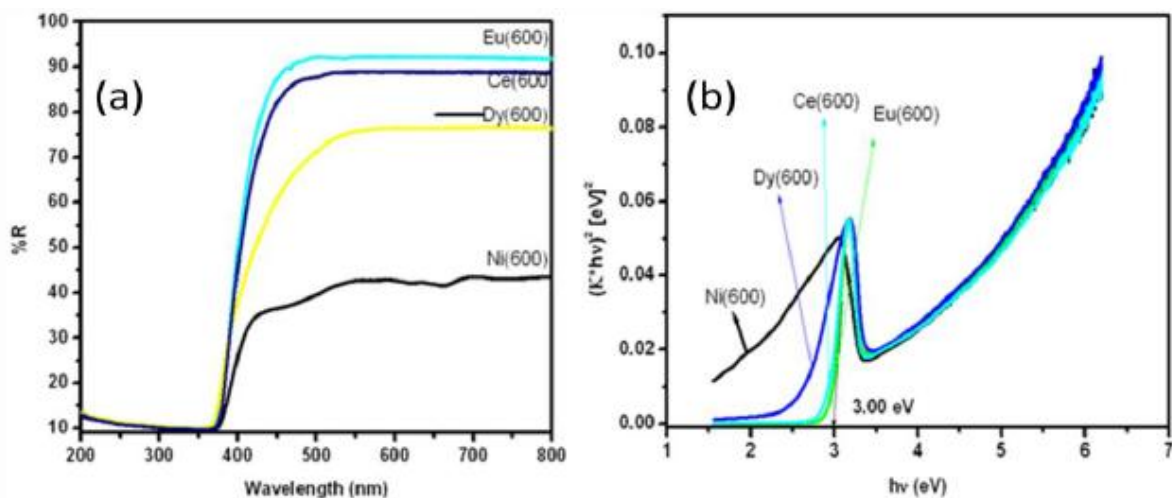


Figure 4: (a) Uv-Vis reflectance and (b) band gap energy spectra of annealed Ce, Dy, Eu and Ni-doped ZnO nanoparticles

4. Conclusion

In summary, the presented data suggest optical-structural correlations in nanosized undoped and doped ZnO materials in terms of crystallinity, defects, and quantum confinement. These properties were revealed by the XRD, SEM, UV-Vis and PL measurements. The incorporation of dopants can influence the morphology of ZnO nanostructures due to defect formation and, consequently, the intensity of the light emission. The effect of post-growth annealing on the structural properties of the nanostructures was determined to lead to an improvement in the crystalline quality. The strong UV and weak green bands emission imply a good optical quality. These results show a great promise for the application of annealed and doped ZnO nanoparticles with low expense and good quantities of electronic and optical properties.

Acknowledgements

Financial support from the National Research Foundation (NRF) of the government of South Africa and the services of the research equipment of University of Free State, Physics department used in this study are gratefully acknowledged by the authors.

References

- [1] Liu Y, Yang J H, Guan Q F, Yang L L, Zhang Y J, Wang Y X, Feng B, Cao J, Liu X Y, Yang Y T, Wei M B, 2009 *J. Alloys Compd.*, **486** 835.
- [2] Wang D Y, Zhou J, Liu G Z, 2009 *J. Alloys Compd.*, **481** 802.
- [3] Reynolds D C, Look D C, Jogai B and Morkoç H, 1997 *Solid State Commun.* **101** 643
- [4] Leverenz V W, An Introduction to Luminescence of Solids, Dover, New York, 1968.
- [5] Xiong G, Wilkinson J, Mischuck B, Tuzemen S, Ucer K B and Williams R T , 202 *Appl. Phys. Lett.* **80** 1195
- [6] Ma Y, Du G T, Yang S R, Li Z T, B. Zhao J, Yang X T, Yang T P, Zhang Y T and Liu D, 2004 *J. Appl. Phys.* **95** 6268
- [7] Oh M-S, Kim S-H and Seong T-Y, 2005 *Appl. Phys. Lett.* **87** 103
- [8] Tan S T, Sun X W, Zhang X H, Chua S J, Chen B J, Teo C C, 2006 *J. Appl. Phys.* **100** 033502
- [9] Chandrasekhar S, 1943 *Rev. Mod. Phys.* **15** 1
- [10] Ahn C H, Kim Y Y, Kim D C, Mohanta S, K, Cho H K 2009 *J. Appl. Phys.* **105** 013502
- [11] J. Lee, A.J. Easteal, U. Pal, D. Bhattacharyy, 2009 *Current Applied Physics*, **9** 792–796.
- [12] Bhargava, R N, Chhabra V, Som T, Ekimov A, Taskar, N. *Phys.* **2002 Status Solidi B** **229** 897
- [13] Koao L F, Swart H C, Coetsee E, Biggs M M, Dejene F B, 2009 *Physica B*, **404** 4499 –4503.
- [14] Z. Wang, H. Zhang, L. Zhang, J. Yuan, C. Wang, 2003 *Nanotechnology* **14** 11.